

1 **Increased large-scale convective aggregation in CMIP5**
2 **projections: implications for tropical precipitation**
3 **extremes**

4 **Carl P. O. Blackberg^{1,2}, Martin S. Singh^{1,2}**

5 ¹School of Earth, Atmosphere, and Environment, Monash University, Victoria, Australia

6 ²Centre of Excellence for Climate Extremes, Monash University, Victoria, Australia

7 **Key Points:**

- 8 • According to three separate metrics, large-scale convective aggregation increases
9 with warming in 17 of 19 global climate models examined.
10 • There is substantial spread in large-scale convective aggregation behavior among
11 the global climate models considered.
12 • No statistically significant inter-model relationship between degree of aggregation
13 and tropical-mean precipitation extremes was found.

Corresponding author: Carl P. O. Blackberg, carlphiliposcar@gmail.com

Abstract

Convective aggregation refers to the clustering of convective events and occurs on a wide range of spatial scales. It has been suggested that the behavior of convective aggregation may change under global warming, with potential implications for future changes in precipitation extremes. Here, a novel method to define convective regions of the tropics using gridded daily precipitation data is developed and used to quantify large-scale convective aggregation in an ensemble of global climate models. Applying three separate indices for aggregation, it is found that large-scale convective aggregation increases in 17 of the 19 analyzed models under future warming. However, aggregation is found not to be correlated with tropical-mean precipitation extremes, either climatologically or with respect to the sensitivity to warming. The large model spread in aggregation indices across the ensemble suggests the possible utility of large-scale convective aggregation as a target for model evaluation.

Plain Language Summary

Rainfall in the tropics is not evenly distributed, rather it occurs in clusters of clouds of various sizes and shapes, from a line of thunderstorms to “superclusters” spanning thousands of km. The size and spatial distribution of these clusters are hypothesized to influence the frequency and intensity of heavy rainfall in the tropics. In this study, we develop a method for quantifying the amount of clustering in the tropics, and we investigate whether it is projected to change in the future in a suite of state-of-the-art climate models. Almost all the models project increases in clustering in the future, but, surprisingly, a model’s projection of clustering does not seem to affect its projection of changes to heavy rainfall. The results suggest that effects other than clustering play a dominant role in determining the range of heavy rainfall outcomes projected by climate models.

1 Introduction

Organized convection in the tropics strongly affects radiative feedbacks, the large-scale circulation and moisture distribution, and the hydrological cycle (Hartmann et al., 1984). Understanding how the organization of convection might change under global warming is therefore crucial to understanding the future large-scale climate. Organized deep convection is characterized by multiple deep convective cells combining to form coherent structures such as squall lines (~ 10 km; Houze Jr., 1977), mesoscale convective complexes (~ 100 km; Maddox, 1980), or tropical cyclones (~ 1000 km; Chavas & Emanuel, 2010). On even larger scales, organization can include the clumping and clustering of these convective systems and their associated precipitation. Such clustering, which we will refer to as “large-scale convective aggregation”, may be associated with long-lived “superclusters” (~ 10000 km; Mapes & Houze Jr., 1993), or stationary features such as the intertropical convergence zone.

Recent studies have suggested that changes in the degree of convective organization at various scales may be an important driver of future changes in precipitation extremes (e.g., Pendergrass et al., 2016; Pendergrass, 2020; Bao et al., 2017). In this paper, we investigate this hypothesis by examining the relationship between large-scale convective aggregation and tropical precipitation extremes in historical simulations and future projections using 19 global climate models (GCMs) from phase 5 of the Coupled Model Intercomparison Project (CMIP5).

Interest in convective aggregation has recently grown out of studies using cloud-permitting models in the idealized setting of radiative-convective equilibrium (RCE; Held et al., 1993; Tompkins & Craig, 1998; Bretherton et al., 2005). Simulations of RCE in a homogeneous domain with no imposed shear or lateral energy transport were found to spontaneously develop organization in a process termed “self-aggregation”. In regional-

63 scale domains, the aggregated state is characterized by a single region of convective ac-
64 tivity surrounded by a dry, quiescent atmosphere, and its development is driven by feed-
65 backs between convection, surface fluxes, and radiation, with longwave radiation being
66 particularly important (Wing & Emanuel, 2014). Simulations of RCE in both global or
67 quasi-global convection-permitting models (Wing & Cronin, 2016; Wing et al., 2018) and
68 in GCMs (Popke et al., 2013; Reed et al., 2015) show evidence of self-aggregation on plan-
69 etary scales, producing multiple convective regions spanning thousands of km across. While
70 GCMs do not resolve the convective-scale processes that lead to mesoscale organization,
71 their tendency to produce large-scale convective aggregation has been argued to be a re-
72 sult of similar feedbacks to those operating in cloud-permitting models (Wing et al., 2017).
73 These feedbacks are also thought to play an important role in driving observed convec-
74 tive systems such as tropical cyclones (Carstens & Wing, 2020) and the Madden-Julian
75 Oscillation (Arnold & Randall, 2015).

76 While self-aggregation in both cloud-permitting models and GCMs is known to be
77 sensitive to details of the model configuration such as the dynamical core, parameter-
78 izations, domain size, and geometry, the tendency for the simulated atmosphere to ag-
79 gregate is often found to increase with temperature (Bony et al., 2016; Wing & Emanuel,
80 2014; Wing et al., 2017). Furthermore, researchers suggest that changes in the degree
81 of aggregation of convection may be related to changes in the intensity of precipitation
82 extremes under global warming (Pendergrass et al., 2016). Increasing trends in precip-
83 itation extremes are observed (Westra et al., 2013) and projected by GCMs (Bador et
84 al., 2018), but the sensitivity of precipitation extremes to warming varies across mod-
85 els, particularly in the tropics (O’Gorman, 2012, 2015). While it is known that this model
86 spread is related to the dynamics of precipitation extreme events (O’Gorman & Schnei-
87 der, 2009), the precise mechanisms that drive it, and the possible role played by convec-
88 tive organization, remains unclear. Studies have highlighted the importance of the de-
89 gree of aggregation in determining precipitation extremes (Bao & Sherwood, 2019) and
90 their sensitivity to warming (Bao et al., 2017) in idealized models. But the role of con-
91 vective aggregation in more realistic settings has yet to be fully explored.

92 Observations also point to a role for convective aggregation in influencing the large-
93 scale atmospheric state. For example, Tobin et al. (2013) found using satellite observa-
94 tions that regions with a higher degree of convective aggregation are accompanied by a
95 drying of the mean state atmosphere (see also Holloway et al., 2017). However, observ-
96 ing trends in convective aggregation remains challenging due to the limited extent and
97 quality of historical records and the large variability and low frequency of events most
98 relevant for aggregation (Knutson et al., 2010; C. Jones & Carvalho, 2006). Neverthe-
99 less, Tselioudis et al. (2010) used satellite observations to identify trends toward an in-
100 creased frequency of organized convection with warming, while Zelinka & Hartmann (2010)
101 showed that the fractional anvil cloud area decreases as a response to increases in trop-
102 ical mean temperature, which is another feature commonly associated with self-aggregation
103 in simulations of RCE (Emanuel et al., 2014; Bony et al., 2016). Finally, Tan et al. (2015)
104 found that a large fraction of the observed trends in regional precipitation in the trop-
105 ics could be associated with the change in frequency of organized convection. However,
106 trends in precipitation extremes have not yet been associated with changes in the organ-
107 ization of convection based on observations.

108 In this study, we seek to bridge the gap between idealized studies relating convec-
109 tive aggregation to precipitation extremes in RCE and the observational work described
110 above by investigating large-scale convective aggregation in simulations with comprehen-
111 sive GCMs. Specifically, we introduce a novel method for defining convectively active
112 regions in the tropics, and we apply it to quantify large-scale convective aggregation in
113 an ensemble of CMIP5 models and in observations from the Global Precipitation Cli-
114 matology Project (GPCP). Based on this quantification, we investigate how large-scale

115 convective aggregation is projected to change in the future, and what implications such
 116 changes may have for precipitation extremes.

117 2 Simulations and precipitation extremes

118 Our analysis is based on 19 GCMs participating in CMIP5 (table S1; Taylor et al.,
 119 2012), chosen by selecting one model from each modeling centre for which the desired
 120 data was available. We used 30-year periods from the historical (1970-2000) and repre-
 121 sentative concentration pathway 8.5 (RCP8.5; 2070-2100) scenarios to represent histor-
 122 ical and future climates, respectively. Precipitation extremes and large-scale convective
 123 aggregation were quantified based on daily precipitation accumulations in the tropical
 124 region (30°S-30°N). To ensure comparability across models, we applied a first-order con-
 125 servative interpolation following P. W. Jones (1999) to a common 2.8×2.8 degree grid
 126 prior to the analysis. Differences between the historical and RCP8.5 scenarios may be
 127 expressed per kelvin warming by dividing by the change in tropical- and time-mean sur-
 128 face air temperature between the relevant periods. Finally, as an observed reference point
 129 for the results from the historical climate, satellite-based estimates of daily precipitation
 130 from the GPCP (v1.3; Huffman et al., 2001) for the years 2007-2017 were regridded to
 131 the same 2.8 × 2.8 degree grid and analyzed using the same methodology.

132 To relate tropical precipitation extremes to the degree of large-scale convective ag-
 133 gregation, we define an overall metric of precipitation extremes across the tropics. This
 134 may be done in a number of ways. Here we take the annual maximum daily precipita-
 135 tion accumulation at each gridpoint (Rx1day; Zhang et al., 2011; Alexander et al., 2019)
 136 and then take the time mean over the relevant 30-year period and the spatial mean over
 137 the tropical region. We refer to this metric as the tropical-mean Rx1day. Conclusions
 138 about the relationship between precipitation extremes and aggregation are unaffected
 139 by taking a longer timescale extreme (Rx5day) or by defining extremes based on a per-
 140 centile calculated over all tropical gridpoints (99th, 99.9th, or 99.99th). We plot results
 141 for changes in tropical-mean precipitation extremes as a percentage change per kelvin
 142 tropical warming, but once again, our main conclusions remain the same if we use ab-
 143 solute changes in precipitation extremes rather than relative ones.

144 Figure 1a-d shows the time-mean value of Rx1day in the historical climate for three
 145 models with varying intensity of precipitation extremes and for the GPCP observations.
 146 The magnitude of precipitation extremes varies distinctly between models, and this vari-
 147 ation is well-captured by the tropical-mean Rx1day metric (Fig. 2a). Overall, the model
 148 spread in tropical-mean Rx1day in the historical climate is considerable; the interquar-
 149 tile range is $\sim 33\text{-}48 \text{ mm day}^{-1}$, encompassing the GPCP observational estimate. But
 150 this range widens to $\sim 20\text{-}82 \text{ mm day}^{-1}$ when all 19 models are considered.

151 As for its climatological value, the fractional change in the tropical-mean Rx1day
 152 with warming also varies considerably across models (Figure 2b), with an interquartile
 153 range spanning $\sim 4.2\text{-}7.5 \text{ \%}/\text{K}$, and a maximum range spanning ($\sim 1\text{-}12.5\%/\text{K}$). This is
 154 consistent with the recent analysis of Bador et al. (2018) using a larger ensemble of CMIP5
 155 models. Notably, the models that have the largest climatological value of the tropical-
 156 mean Rx1day (e.g., bcc-csm1-1) are not necessarily the same models that produce the
 157 largest fractional sensitivity per kelvin warming (e.g., IPSL-CM5A-MR). Further, un-
 158 like for the climatology, the spatial pattern of changes in Rx1day with warming also varies
 159 considerably across models (Fig. 3e-g), demonstrating a limitation in using a single tropics-
 160 wide metric for changes in precipitation extremes. Despite this caveat, the large model
 161 spread in tropical-mean Rx1day and its changes with warming imply fundamental dif-
 162 ferences in the representation of precipitation extremes across the ensemble. Our aim
 163 is to determine whether this model spread may be explained by differences in large-scale
 164 convective aggregation in the simulations.

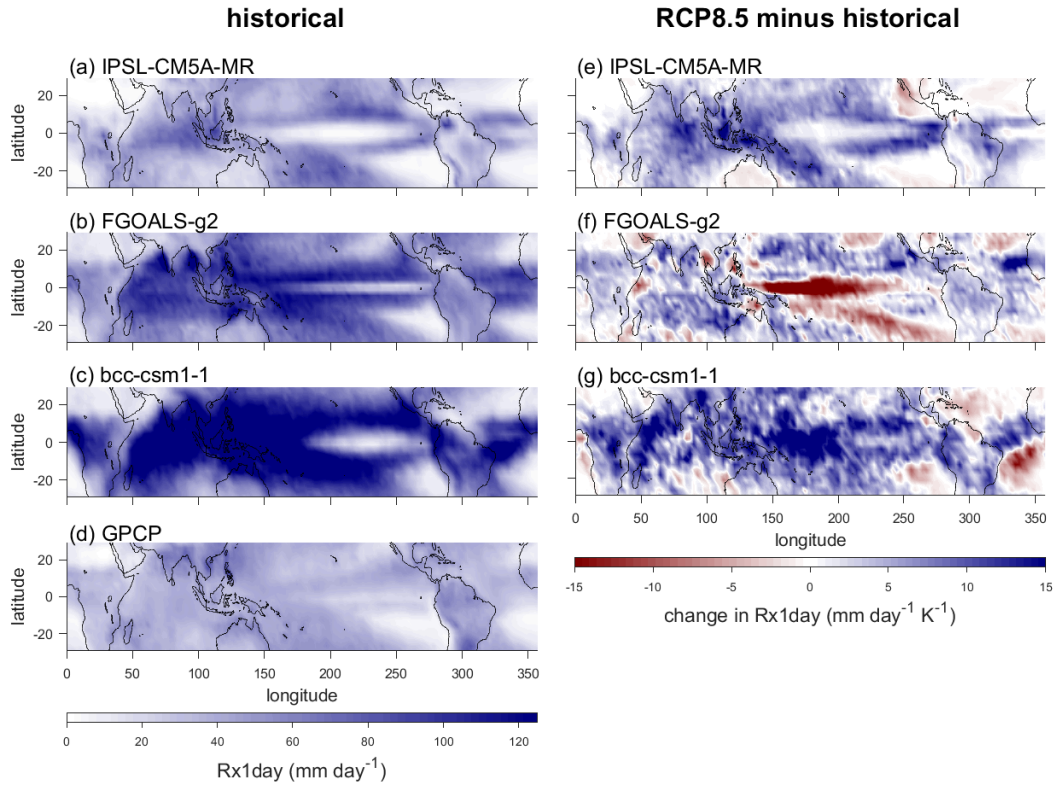


Figure 1. (a-c) Time-mean Rx1day in the historical (1970-2000) scenario and (e-g) change in time-mean Rx1day between the historical and RCP8.5 (2070-2100) scenarios for three CMIP5 models as labelled. Panel (d) gives observational estimate of time-mean Rx1day according to GPCP for the years 2007-2017.

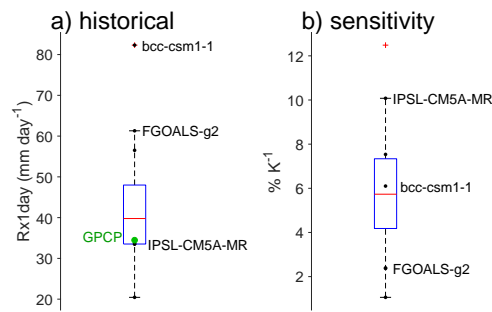


Figure 2. Box-whisker plots of (a) tropical-mean Rx1day in the historical (1970-2000) scenario and (b) fractional increase in tropical-mean Rx1day between the historical and RCP8.5 (2070-2100) scenarios expressed per kelvin of tropical warming for the CMIP5 ensemble. Example models from Fig. 1 are shown as labelled, and GPCP observations are shown in panel (a) in green.

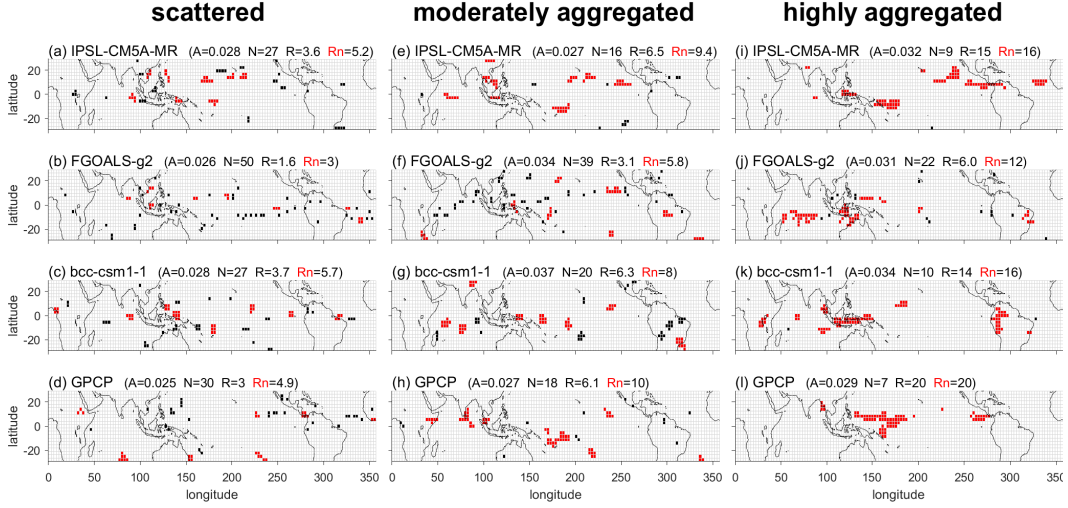


Figure 3. Spatial distribution of convective regions for the minimum (a-d), median (e-h), and maximum (i-l) value of ROME from daily scenes in the historical scenario for the same models as in Fig. 1 and for the GPCP observations as labelled. Each panel includes value of area fraction of convective regions in the scene (A), Number Index (N), ROME (R), and ROME based on the eight largest contiguous convective regions (Rn; in red). ROME is given in units of 10^5 km^2

3 Quantifying large-scale convective aggregation

In order to quantify the degree of large-scale convective aggregation across the tropics, we first define whether a given gridpoint is “convective”. Previous studies have used a range of variables to define regions of active convection such as cloud amount, vertical velocity, outgoing longwave radiation, and precipitation (e.g., Tobin et al., 2012; Tompkins & Semie, 2017; Holloway, 2017). To facilitate comparison with precipitation extremes, here we take gridpoints for which the daily precipitation rate exceeds a threshold value to be convective gridpoints. Since the overall precipitation intensity may vary across models and with climate, we use a separate threshold for each simulation and for the observations to allow for a more robust quantification of large-scale convective aggregation. Specifically, the precipitation threshold is defined as the 97th percentile precipitation rate (including all tropical gridpoints) for each GCM and respective scenario and for the observations. Choosing such a threshold ensures that we identify high precipitation rates in relation to each model’s dynamics and that we roughly pick out the same convective area fraction across the tropics each day. Comparing a similar day-to-day area fraction greatly reduces bias in the aggregation assessment (Tobin et al., 2012).

Convective aggregation may loosely be described as the “coming together” or clustering of convective regions; however, it does not currently have a strict quantifiable definition (Weger et al., 1992; Retsch et al., 2020). Nevertheless, it is generally agreed that the degree of convective aggregation increases with the size and proximity of contiguous convective regions (Tobin et al., 2012; White et al., 2018). More generally, convective organization may also depend on other considerations such as the shape, pattern, timing, and general spatial distribution of convective regions (Pendergrass et al., 2016; Retsch et al., 2020).

In this study, we consider contiguous regions of convection as 8-connected convective grid points, and we use three simple metrics of varying approaches to quantify the large-scale aggregation of convection in the tropics as a whole. For a fixed area fraction

192 of convection, we expect aggregation to increase with the size and decrease with the num-
 193 ber of contiguous convective regions. Therefore, as the first measure of aggregation, we
 194 analyze the Precipitation Weighted Area Distribution (PWAD). The PWAD describes
 195 the fraction of tropical precipitation that falls in contiguous convective regions of a given
 196 size. Here size is quantified by the effective radius $r_{\text{eff}} = \sqrt{a/\pi}$, of a continuous con-
 197 vective region of area a . A shift in the PWAD from smaller to larger values of effective
 198 radius corresponds to an increase in aggregation.

199 A second, more quantitative, measure of large-scale convective aggregation is given
 200 by the average number of contiguous convective regions in a daily tropical scene, which
 201 we refer to as the Number Index. Considering that our definition identifies convection
 202 as occupying roughly the same area fraction of the tropics each day, a decrease in the
 203 number of contiguous convective regions is likely to correspond to an increase in the av-
 204 erage size of these regions and an increase in the degree of aggregation.

205 Finally, as a third measure of large-scale convective aggregation, we use a slightly
 206 more sophisticated aggregation index, the Radar Organisation METric (ROME), which
 207 considers the average size, proximity, and size distribution of contiguous convective re-
 208 gions (Retsch et al., 2020). As its name suggests, ROME was originally designed for anal-
 209 ysis of radar observations, but we find that it works well for our purposes. ROME as-
 210 sesses organisation by defining “connections” between pairs of continuous convective re-
 211 gions and assigning a weight to each pair that increases with their respective areas and
 212 decreases with their separation distance. Specifically, the weight is equal to the area of
 213 the larger contiguous convective region plus a contribution from the smaller contiguous
 214 convective region that depends on the separation distance. For a given scene, ROME is
 215 then taken as the average value of the weights for all pairs of contiguous convective re-
 216 gions in the tropics. ROME is measured in units of area, and its value may be decom-
 217 posed into a contribution from the mean area of contiguous convective regions and a con-
 218 tribution that depends on the distribution of sizes of and interaction between different
 219 contiguous convective regions (Retsch et al., 2020). An increasing value of ROME cor-
 220 responds to a higher degree of aggregation.

221 Analysis of daily precipitation distributions in different models reveals that the ag-
 222 gregation assessment from the Number Index and ROME can sometimes be skewed by
 223 a large number of isolated single grid points of convection. Such “gridpoint storms” are
 224 known non-physical features of GCM-simulated precipitation distributions (Pendergrass
 225 & Hartmann, 2014). To account for the potential bias introduced by such effects, ROME
 226 was also calculated based on the eight largest contiguous convective regions in each daily
 227 scene (shown in red in Fig. 3).

228 Examples of daily scenes from different GCMs under the historical scenario and
 229 from the GPCP observations reveal that the various aggregation indices correspond well
 230 to a subjective visual assessment of large-scale convective aggregation (Fig. 3). As ag-
 231 gregation according to ROME and the Number Index increase, the size of contiguous con-
 232 vective regions becomes larger, and their distribution more clustered. Both the obser-
 233 vations and GCMs exhibit a wide range of ROME values, demonstrating substantial tem-
 234 poral variability in large-scale convective aggregation across the tropics.

235 All three approaches analyzed reveal considerable model spread in the simulated
 236 large-scale convective aggregation in the historical scenario. The ensemble-mean PWAD
 237 peaks at r_{eff} in the range 343-515 km and is very similar to that observed by GPCP, but
 238 certain models exhibit substantially different behavior (Fig. 3a). For example, FGOALS-
 239 g2 generates much greater numbers of small contiguous convective regions, while bcc-
 240 csm1-1 tends to predominantly generate contiguous convective regions of medium size.
 241 Additionally, the mean values of ROME and Number Index in the historical scenario vary
 242 from roughly half to almost double that of the GPCP observational estimate (Fig. 4c).

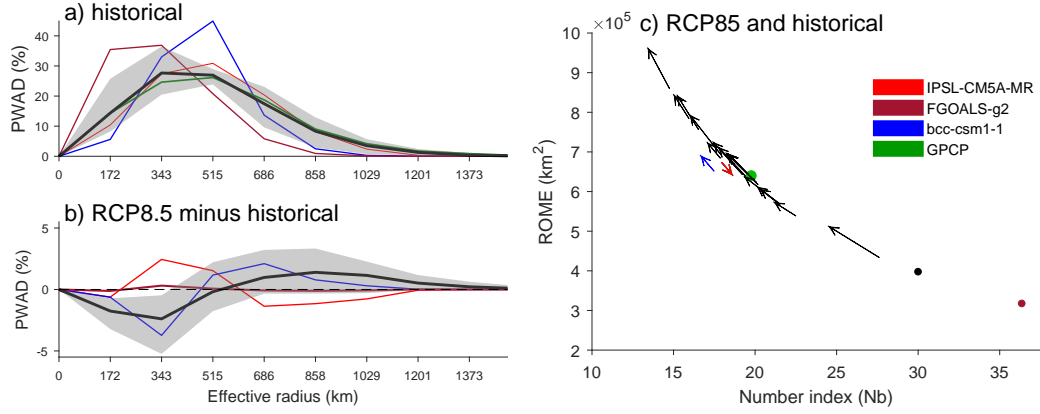


Figure 4. (a) Precipitation-weighted area distribution (PWAD) in the historical scenario and for the GPCP observations (green) and (b) difference in PWAD between the RCP8.5 and historical scenarios. Black line gives ensemble mean and gray shading shows range of 90% of GCMs. Colored lines show example models as labelled in (c). PWAD is calculated using bins with width equal to the mean effective radius of tropical gridboxes. (c) Mean Number index plotted against mean ROME for historical (base of the arrow) and RCP8.5 (tip of the arrow) scenario for each GCM in the ensemble. Dots are used for the GPCP observations and for GCMs with little change in aggregation.

243 This large model spread points to the possible utility of such metrics of large-scale convective aggregation for model evaluation.
244

245 We now consider how aggregation changes under warming. All metrics agree that
246 the same 17 of the 19 considered GCMs exhibit an increase in the degree of large-scale
247 convective aggregation in the RCP8.5 scenario. In these GCMs, The PWAD tends to shift
248 from smaller to larger contiguous convective regions (Figure 4b), the average number of
249 objects in each daily scene decreases (Figure 4c), and the average ROME value increases
250 with warming (Figure 4c). In the remaining two models, IPSL-CM5A-MR shows a decrease
251 in aggregation according to all metrics, while FGOALS-g2 shows small changes
252 in aggregation whose sign depends on the choice of metric. We also repeated these calculations
253 with precipitation thresholds for convective regions based on different percentiles
254 (95th, 97th, and 99th percentile) and for ROME calculated using only the largest 8 contiguous
255 convective regions, and while the absolute value of the aggregation metrics is altered,
256 the trend with warming is consistent with the results shown here.

257 4 Relationship between large-scale convective aggregation and precipitation extremes 258

259 Previous researchers have found changes in convective aggregation to be an important
260 determinant of changes in precipitation extremes in idealized simulations of RCE
261 (e.g., Bao et al., 2017). However, our analysis reveals no statistically significant relationship
262 between the degree of large-scale convective aggregation, as measured by ROME,
263 and precipitation extremes, as measured by tropical-mean Rx1day, for either their climatological
264 values (Figure 5a) or their changes with warming (Figure 5b) across the 19 GCMs considered.
265 This result holds for any combination of the analyzed large-scale convective aggregation
266 metrics and precipitation extremes metrics described above. Thus while the intensity of precipitation
267 extremes increases with warming for all models and the degree of convective aggregation
268 increases with warming in most models, our results

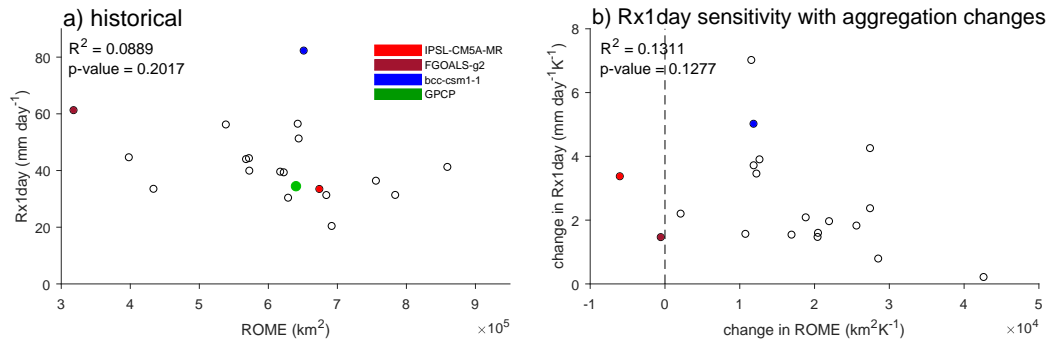


Figure 5. Scatter plot of (a) tropical-mean Rx1day vs ROME for GCMs under the historical scenario and in GPCP observations (green) and (b) difference in tropical-mean Rx1day and ROME from historical to RCP8.5 scenario per kelvin of tropical warming.

269 do not support a role for changes in large-scale convective aggregation in modulating pre-
 270 cipitation extremes, at least at a tropics-wide level.

271 5 Conclusions

272 We have examined projected changes to large-scale convective aggregation and pre-
 273 cipitation extremes as simulated by 19 GCMs under the RCP8.5 scenario. We have used
 274 a novel method to identify convective regions based on a percentile precipitation thresh-
 275 old that ensures a roughly fixed fraction of the tropics is identified as convective. This
 276 method allows for a robust quantification of the degree of large-scale convective aggre-
 277 gation in the tropics as a whole that is consistent across a range of metrics. Broadly con-
 278 sistent with previous RCE studies (Bony et al., 2016; Wing et al., 2018), we find that,
 279 in most models, large-scale convective aggregation increases with warming. However, we
 280 find no evidence that changes in aggregation are linked to changes in precipitation ex-
 281 tremes across the GCM ensemble, at least for our tropics-wide measures of aggregation
 282 and precipitation extremes. This contrasts with previous studies of RCE, for which changes
 283 to convective aggregation appear to be an important driver of changes in precipitation
 284 extremes under warming, at least in the context of experiments with a single model (Pen-
 285 dergrass et al., 2016; Bao et al., 2017).

286 An important caveat to our work is that we examine convective aggregation in mod-
 287 els with parameterized convection. Such models do not resolve the processes that lead
 288 to organization of convection on mesoscales, and this may affect how they simulate large-
 289 scale convective aggregation. Indeed, we show that there is considerable model spread
 290 in the degree of large-scale convective aggregation in the GCM ensemble, with some mod-
 291 els displaying distinctly different aggregation behavior from the bulk of the models and
 292 from the observations. In previous idealized studies, the choice of convection parame-
 293 terization has been shown to have a large effect on large-scale convective aggregation (Bao
 294 et al., 2017), and this provides one explanation for the anomalous behaviour seen in some
 295 of the CMIP5 models. Investigation into the specific model configurations and param-
 296 eterizations relevant for large-scale convective aggregation is needed to confirm these spec-
 297 ulations. Such an endeavour could include categorizing different convection schemes and
 298 investigating which features of parameterizations promote or suppress aggregation (Mon-
 299 crieff, 2019).

300 The large model spread in large-scale convective aggregation also suggests that it
 301 may provide a useful target for model evaluation. While we provide a preliminary as-

302 assessment of observed large-scale convective aggregation using GPCP data, further work
 303 in quantifying the observed uncertainties are required before this could be used for more
 304 formal model evaluation.

305 While our results do not show a relationship between simulated tropical precipi-
 306 tation extremes and large-scale convective aggregation for the tropics as a whole, the ex-
 307 tent to which such relationships may exist at a regional level, or for more general mea-
 308 sures of convective organization remains an open question. Possible future work to ad-
 309 dress this question could include analysis of specific geographical areas with distinct cli-
 310 matologies, and development of metrics that look at specific convective shapes (e.g., con-
 311 vergence lines; Weller et al., 2017). Alternatively, the reasons for the lack of a tropics-
 312 wide relationship between precipitation extremes and large-scale convective aggregation
 313 might be ascertained by tracking precipitation extremes in individual storms or events
 314 that are impacted by convective aggregation (Pendergrass et al., 2016).

315 Other considerations for further investigation include analysis of the tropospheric
 316 humidity distribution. In RCE, aggregation is characterized by an increased variance of
 317 humidity (Wing & Emanuel, 2014), and from both simulations and observations, aggrega-
 318 tion is accompanied by a drying of the mean state atmosphere (Holloway et al., 2017).
 319 This suggests that simulated changes in large-scale convective aggregation may affect fu-
 320 ture projections of tropospheric humidity.

321 Acknowledgments

322 We acknowledge the World Climate Research Programme’s Working Group on Coupled
 323 Modelling, which is responsible for CMIP, and we thank the climate modeling groups
 324 (listed in Table S1 of this paper) for producing and making available their model out-
 325 put. Model output used in this paper is available through the U.S. Department of En-
 326 ergy’s Program for Climate Model Diagnosis and Intercomparison at [https://pcmdi.llnl.gov/mips/cmip5/data-](https://pcmdi.llnl.gov/mips/cmip5/data-portal.html)
 327 [portal.html](https://pcmdi.llnl.gov/mips/cmip5/data-portal.html). The GPCP precipitation dataset is available at [https://doi.org/10.5065/ZGJD-](https://doi.org/10.5065/ZGJD-9B02)
 328 [9B02](https://doi.org/10.5065/ZGJD-9B02). We acknowledge support from the Australian Research Council through grant no.
 329 DE190100866 and through the Centre of Excellence for Climate Extremes (grant no. CE170100023)
 330 and computational resources and services from the National Computational Infrastruc-
 331 ture, all funded by the Australian Government.

332 References

- 333 Alexander, L. V., Fowler, H. J., Bador, M., Behrangi, A., Donat, M. G., Dunn, R.,
 334 ... Venugopal, V. (2019). On the use of indices to study extreme precipitation on
 335 sub-daily and daily timescales. *Environmental Research Letters*, *14*(12), 125008.
 336 doi: 10.1088/1748-9326/ab51b6
- 337 Arnold, N. P., & Randall, D. A. (2015). Global-scale convective aggregation: Impli-
 338 cations for the Madden-Julian Oscillation. *Journal of Advances in Modeling Earth*
 339 *Systems*, *7*(4), 1499-1518. doi: 10.1002/2015MS000498
- 340 Bador, M., Donat, M. G., Geoffroy, O., & Alexander, L. V. (2018). Assessing the
 341 robustness of future extreme precipitation intensification in the CMIP5 ensemble.
 342 *Journal of Climate*, *31*(16). doi: 10.1175/JCLI-D-17-0683.1
- 343 Bao, J., & Sherwood, S. C. (2019). The role of convective self-aggregation in ex-
 344 treme instantaneous versus daily precipitation. *Journal of Advances in Modeling*
 345 *Earth Systems*, *11*(1), 19-33. doi: 10.1029/2018MS001503
- 346 Bao, J., Sherwood, S. C., Colin, M., & Dixit, V. (2017). The robust relationship
 347 between extreme precipitation and convective organization in idealized numerical
 348 modeling simulations. *Journal of Advances in Modeling Earth Systems*, *9*(6),
 349 2291-2303. doi: 10.1002/2017MS001125
- 350 Bony, S., Stevens, B., Coppin, D., Becker, T., Reed, K. A., Voigt, A., & Medeiros,
 351 B. (2016). Thermodynamic control of anvil cloud amount. *Proceedings of the Na-*

- 352 *tional Academy of Sciences*, 113(32), 8927–8932. doi: 10.1073/pnas.1601472113
- 353 Bretherton, C. S., Blossey, P. N., & Khairoutdinov, M. (2005). An energy-balance
354 analysis of deep convective self-aggregation above uniform SST. *Journal of the At-*
355 *mospheric Sciences*, 62(12), 4273 - 4292. doi: 10.1175/JAS3614.1
- 356 Carstens, J. D., & Wing, A. A. (2020). Tropical cyclogenesis from self-aggregated
357 convection in numerical simulations of rotating radiative-convective equilibrium.
358 *Journal of Advances in Modeling Earth Systems*, 12(5), e2019MS002020. doi:
359 10.1029/2019MS002020
- 360 Chavas, D. R., & Emanuel, K. A. (2010). A QuikSCAT climatology of tropical cy-
361 clone size. *Geophysical Research Letters*, 37(18). doi: 10.1029/2010GL044558
- 362 Emanuel, K., Wing, A. A., & Vincent, E. M. (2014). Radiative-convective instabil-
363 ity. *Journal of Advances in Modeling Earth Systems*, 6(1), 75-90. doi: 10.1002/
364 2013MS000270
- 365 Hartmann, D. L., Hendon, H. H., & Houze Jr., R. A. (1984). Some implications
366 of the mesoscale circulations in tropical cloud clusters for large-scale dynam-
367 ics and climate. *Journal of the Atmospheric Sciences*, 41(1), 113 - 121. doi:
368 10.1175/1520-0469(1984)041<0113:SIOTMC>2.0.CO;2
- 369 Held, I. M., Hemler, R. S., & Ramaswamy, V. (1993). Radiative-convective equilib-
370 rium with explicit two-dimensional moist convection. *Journal of Atmospheric Sci-*
371 *ences*, 50(23), 3909 - 3927. doi: 10.1175/1520-0469(1993)050<3909:RCEWET>2.0
372 .CO;2
- 373 Holloway, C. E. (2017). Convective aggregation in realistic convective-scale simula-
374 tions. *Journal of Advances in Modeling Earth Systems*, 9(2), 1450–1472. doi: 10
375 .1002/2017MS000980
- 376 Holloway, C. E., Wing, A. A., Bony, S., Muller, C., Masunaga, H., L’Ecuyer,
377 T. S., ... Zuidema, P. (2017). Observing convective aggregation. In R. Pin-
378 cus, D. Winker, S. Bony, & B. Stevens (Eds.), *Shallow clouds, water va-*
379 *por, circulation, and climate sensitivity* (Vol. 65, p. 27-64). Springer. doi:
380 10.1007/978-3-319-77273-8_2
- 381 Houze Jr., R. A. (1977). Structure and dynamics of a tropical squall–line
382 system. *Monthly Weather Review*, 105(12), 1540 - 1567. doi: 10.1175/
383 1520-0493(1977)105<1540:SADOAT>2.0.CO;2
- 384 Huffman, G. J., Adler, R. F., Morrissey, M. M., Bolvin, D. T., Curtis, S., Joyce,
385 R., ... Susskind, J. (2001). Global precipitation at one-degree daily resolution
386 from multisatellite observations. *Journal of Hydrometeorology*, 2(1), 36 - 50. doi:
387 10.1175/1525-7541(2001)002<0036:GPAODD>2.0.CO;2
- 388 Jones, C., & Carvalho, L. M. V. (2006). Changes in the activity of the Mad-
389 den–Julian Oscillation during 1958–2004. *Journal of Climate*, 19(24), 6353 - 6370.
390 doi: 10.1175/JCLI3972.1
- 391 Jones, P. W. (1999). First- and second-order conservative remapping schemes for
392 grids in spherical coordinates. *Monthly Weather Review*, 127(9), 2204 - 2210. doi:
393 10.1175/1520-0493(1999)127<2204:FASOCR>2.0.CO;2
- 394 Knutson, T. R., McBride, J. L., Chan, J., Emanuel, K., Holland, G., Landsea, C.,
395 ... Sugi, M. (2010). Tropical cyclones and climate change. *Nature Geoscience*, 3,
396 157–163. doi: 10.1038/ngeo779
- 397 Maddox, R. A. (1980). Mesoscale convective complexes. *Bulletin of the American*
398 *Meteorological Society*, 61(11), 1374–1387.
- 399 Mapes, B. E., & Houze Jr., R. A. (1993). Cloud clusters and superclusters over the
400 oceanic warm pool. *Monthly Weather Review*, 121(5), 1398 - 1416. doi: 10.1175/
401 1520-0493(1993)121<1398:CCASOT>2.0.CO;2
- 402 Moncrieff, M. W. (2019). Toward a dynamical foundation for organized convection
403 parameterization in GCMs. *Geophysical Research Letters*, 46(23), 14103-14108.
404 doi: 10.1029/2019GL085316
- 405 O’Gorman, P. A. (2012). Sensitivity of tropical precipitation extremes to climate

- change. *Nature Geoscience*, 5, 697–700. doi: 10.1038/ngeo1568
- O’Gorman, P. A. (2015). Precipitation extremes under climate change. *Current Climate Change Reports*, 1, 49–59. doi: 10.1007/s40641-015-0009-3
- O’Gorman, P. A., & Schneider, T. (2009). The physical basis for increases in precipitation extremes in simulations of 21st-century climate change. *Proceedings of the National Academy of Sciences of the USA*, 106(35), 14773–14777. doi: 10.1073/pnas.0907610106
- Pendergrass, A. G. (2020). Changing degree of convective organization as a mechanism for dynamic changes in extreme precipitation. *Current Climate Change Reports*, 6, 47–54. doi: 10.1007/s40641-020-00157-9
- Pendergrass, A. G., & Hartmann, D. L. (2014). Changes in the distribution of rain frequency and intensity in response to global warming. *Journal of Climate*, 27(22), 8372–8383. doi: 10.1175/JCLI-D-14-00183.1
- Pendergrass, A. G., Reed, K. A., & Medeiros, B. (2016). The link between extreme precipitation and convective organization in a warming climate: Global radiative-convective equilibrium simulations. *Geophysical Research Letters*, 43(21), 11,445–11,452. doi: 10.1002/2016GL071285
- Popke, D., Stevens, B., & Voigt, A. (2013). Climate and climate change in a radiative-convective equilibrium version of ECHAM6. *Journal of Advances in Modeling Earth Systems*, 5(1), 1–14. doi: 10.1029/2012MS000191
- Reed, K. A., Medeiros, B., Bacmeister, J. T., & Lauritzen, P. H. (2015). Global radiative-convective equilibrium in the Community Atmosphere Model, version 5. *Journal of the Atmospheric Sciences*, 72(5), 2183–2197. doi: 10.1175/JAS-D-14-0268.1
- Retsch, M. H., Jakob, C., & Singh, M. S. (2020). Assessing convective organization in tropical radar observations. *Journal of Geophysical Research: Atmospheres*, 125(7), e2019JD031801. doi: 10.1029/2019JD031801
- Tan, J., Jakob, C., Rossow, W. B., & Tselioudis, G. (2015). Increases in tropical rainfall driven by changes in frequency of organized deep convection. *Nature*, 519, 451–454. doi: 10.1038/nature14339
- Taylor, K. E., Stouffer, R. J., & Meehl, G. A. (2012). An overview of CMIP5 and the experiment design. *Bulletin of the American Meteorological Society*, 93(4), 485–498. doi: 10.1175/BAMS-D-11-00094.1
- Tobin, I., Bony, S., Holloway, C. E., Grandpeix, J.-Y., Sèze, G., Coppin, D., . . . Roca, R. (2013). Does convective aggregation need to be represented in cumulus parameterizations? *Journal of Advances in Modeling Earth Systems*, 5(4), 692–703. doi: 10.1002/jame.20047
- Tobin, I., Bony, S., & Roca, R. (2012). Observational evidence for relationships between the degree of aggregation of deep convection, water vapor, surface fluxes, and radiation. *Journal of Climate*, 25(20), 6885–6904. doi: 10.1175/JCLI-D-11-00258.1
- Tompkins, A. M., & Craig, G. C. (1998). Radiative-convective equilibrium in a three-dimensional cloud-ensemble model. *Quarterly Journal of the Royal Meteorological Society*, 124(550), 2073–2097. doi: 10.1002/qj.49712455013
- Tompkins, A. M., & Semie, A. G. (2017). Organization of tropical convection in low vertical wind shears: Role of updraft entrainment. *Journal of Advances in Modeling Earth Systems*, 9(2), 1046–1068. doi: 10.1002/2016MS000802
- Tselioudis, G., Tromeur, E., Rossow, W. B., & Zerefos, C. S. (2010). Decadal changes in tropical convection suggest effects on stratospheric water vapor. *Geophysical Research Letters*, 37(14), L14806. doi: 10.1029/2010GL044092
- Weger, R. C., Lee, J., Zhu, T., & Welch, R. M. (1992). Clustering, randomness and regularity in cloud fields: 1. Theoretical considerations. *Journal of Geophysical Research: Atmospheres*, 97(D18), 20519–20536. doi: 10.1029/92JD02038
- Weller, E., Shelton, K., Reeder, M. J., & Jakob, C. (2017). Precipitation associated

- 460 with convergence lines. *Journal of Climate*, 30(9), 3169–3183. doi: 10.1175/JCLI
461 -D-16-0535.1
- 462 Westra, S., Alexander, L. V., & Zwiers, F. W. (2013). Global increasing trends
463 in annual maximum daily precipitation. *Journal of Climate*, 26(11), 3904 - 3918.
464 doi: 10.1175/JCLI-D-12-00502.1
- 465 White, B. A., Buchanan, A. M., Birch, C. E., Stier, P., & Pearson, K. J. (2018).
466 Quantifying the effects of horizontal grid length and parameterized convection
467 on the degree of convective organization using a metric of the potential for con-
468 vective interaction. *Journal of the Atmospheric Sciences*, 75(2), 425-450. doi:
469 10.1175/JAS-D-16-0307.1
- 470 Wing, A. A., & Cronin, T. W. (2016). Self-aggregation of convection in long chan-
471 nel geometry. *Quarterly Journal of the Royal Meteorological Society*, 142(694), 1–
472 15. doi: 10.1002/qj.2628
- 473 Wing, A. A., Emanuel, K., Holloway, C. E., & Muller, C. (2017). Convective self-
474 aggregation in numerical simulations: A review. In R. Pincus, D. Winker, S. Bony,
475 & B. Stevens (Eds.), *Shallow clouds, water vapor, circulation, and climate sensi-*
476 *tivity* (Vol. 65, p. 1-25). Springer. doi: 10.1007/978-3-319-77273-8_1
- 477 Wing, A. A., & Emanuel, K. A. (2014). Physical mechanisms controlling self-
478 aggregation of convection in idealized numerical modeling simulations. *Journal of*
479 *Advances in Modeling Earth Systems*, 6(1), 59-74. doi: 10.1002/2013MS000269
- 480 Wing, A. A., Reed, K. A., Satoh, M., Stevens, B., Bony, S., & Ohno, T. (2018). Ra-
481 diative–convective equilibrium model intercomparison project. *Geoscientific Model*
482 *Development*, 11, 793-813. doi: 10.5194/gmd-11-793-2018
- 483 Zelinka, M. D., & Hartmann, D. L. (2010). The observed sensitivity of high clouds
484 to mean surface temperature anomalies in the tropics. *Journal of Geophysical Re-*
485 *search*, 116(D23), D23103. doi: 10.1029/2011JD016459
- 486 Zhang, X., Alexander, L., Hegerl, G. C., Jones, P., Tank, A. K., Peterson, T. C., ...
487 Zwiers, F. W. (2011). Indices for monitoring changes in extremes based on daily
488 temperature and precipitation data. *Wiley Interdisciplinary Reviews: Climate*
489 *Change*, 2, 851-870. doi: 10.1002/wcc.147